HAPTICS SYMPOSIUM '16, APRIL 8–11, 2016, PHILADELPHIA, PENNSYLVANIA, USA
978-1-5090-0903-9/16/$31.00 ©2016 IEEE

A Versatile and Modular Capacitive Tactile Proximity Sensor

Hosam Alagi[1], Stefan Escaida Navarro[1], Michael Mende[1] and Björn Hein[1]

***Abstract*— In this work we discuss the design and realization of a novel capacitive tactile proximity sensor (CTPS) with applications in robotics and consumer-electronics. The current concept is an advancement with respect to a previous design developed at our lab. Experience in the development of applications based on the old sensor, such as manipulation and safe HRI, helped determining the requirements. The new sensor is capable of operating in a self- and mutual-capacitive proximity mode and in a mutual-capacitive tactile mode. The issue of having a trade-off between spatial resolution and sensing range in proximity mode due to the capacitive measurement principle is addressed. A circuit is designed to dynamically select or join electrodes involved in the proximity measurements, a technique which at the same time allows the implementation of the spatial resolution in the tactile mode. Also, all signal processing is done on board of the prototype sensor module, thus complete modularity is achieved.**

I. Introduction

Touch sensors or artificial skins play a significant role in robotics and consumer-electronics where they are used to enable manipulation capabilities and safety features of robotic systems as well as HMI in general. Traditional challenges in their design include implementing an adequate spatial resolution, sufficient touch sensitivity and coverage of large areas as well as integration into confined space, such as in the fingers of grippers. Beyond this, the current work is related to a trend in artificial skin development in which the traditional sense of touch is complemented by further modalities, i.e. *multimodal skins*. On the one hand, some approaches are committed to mimicry of human scale and capabilities, e.g. temperature and vibration sensing. Here, applications also reach into the domain of prosthetics. On the other hand, some approaches are oriented towards improving the sensing capabilities of robots or electronic devices in general without regard for human likeness, e.g. proximity sensing or inertial measurements.

A subset of the approaches consists of the ones combining tactile and proximity sensing. This combination is of special interest to us, because the sense of touch is extended in a way that is naturally useful: no tactile event can occur without a prior proximity event and therefore proximity sensing can be used to enhance robustness of grasping and manipulation methods as well as safety and intuitiveness in HRI. In fact, it has been our line of recent research to investigate the corresponding sensor technology on the one hand [1], [2] and applications in robotics on the other hand. So far, the researched applications have ranged from proximity tracking and contact prediction [3], over preshaping, grasping and haptic exploration [4] to telemanipulation with force-feedback based on proximity sensing [5], [6]. In [5], [6] it has been shown that proximity information can also be intuitively processed by humans when displayed as forces in tele-sensing scenarios.

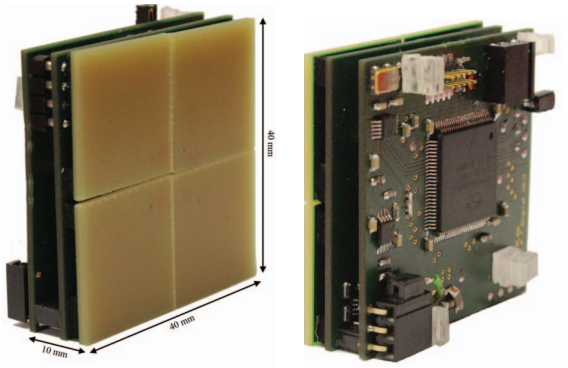

(a) Front side showing the layers of electrodes and foam (b) Back side showing digital electronics

Fig. 1. A prototypical tactile proximity sensor module that shows the concepts discussed in this work

The current work is a direct continuation of the work on sensor design proposed in [1], [2]. We extend this approach by an refined design of the sensing element, which uses less electrode layers to implement the same functionality. Also, our design is novel regarding the implementation of a dynamic spatial resolution for the proximity mode that addresses the issue of having a trade-off between electrode size and sensing range, whereby the first determines the attainable spatial resolution. Finally, we introduce an implementation and a first evaluation of the sensor that is modular, i.e. has digital signal processing on board and can be interconnected with other modules to form a skin. Fig. 1 shows the module that we built to test our concepts.

The remainder of the paper is structured as follows: In the section after this introduction we review the related work from the field. In Sec. III we explain the sensor design from a mechanical and electrical point of view. In Sec. IV we show results for the different operation modes of a prototypical sensor module and in Sec. V we summarize the work and give an outlook for future research directions.

II. Related Work

One example for the trend of multimodal tactile sensors is the *BioTac* sensor by *Syntouch* that is co-designed with

*This research was funded by the German Research Foundation (DFG) under the grants HE 7000/1-1 and WO 720/43-1.

[1]Authors are with Institute for Anthropomatics and Robotics - Intelligent Process Control and Robotics Lab (IAR-IPR), Karlsruhe Institute of Technology {hosam.alagi, stefan.navarro, michael.mende, bjoern.hein}@kit.edu

a fingertip at human scale that includes tactile sensing, measurement of temperature flow and vibration [7]. Another example is the *HEX-o-SKIN* by Mittendorfer et al., being a modular sensor patch containing 3 tactile cells, an infrared transmitter and receiver pair for proximity sensing, a temperature sensor and an inertial measurement system [8]. Additionally, [8] addresses the issue of enabling a large scale skin by connecting single modules via a bus-system.

Regarding tactile proximity sensors specifically, the group of *Shimojo Labs* has recently shown sensor designs for grippers equipped with a network of IR proximity sensors and resistive tactile sensors [9], [10]. With their bimodal sensor they have shown some applications, e.g time to contact-based grasping [10] and more. One of the drawbacks of using IR sensor elements is that it is not trivially possible to concurrently implement tactile sensing at the same location, i.e. there will be a *dead spot* for tactile sensing. Also, while the approach for proximity sensing of Shimojo Labs features extremely low latency ($< 1\,\text{ms}$) it is not capable of detecting multiple events simultaneously.

Approaches using capacitive sensing for both tactile and proximity sensing can avoid dead spots and have some benefits over IR sensing, but also present some challenges. Lee et al. [11] use an arrangement of crossing wires separated by a compressible layer to implement their sensor. Taxels are therefore realized at the crossing points, where a change in capacitance can be measured related to the compression, i.e. the change in distance between the wires. Proximity sensing is realized by joining the stripes from the top layer in two groups in order to implement a mutual-capacitive sensing element in which one group of wires is used to send a current received by the other group. An object in the proximity disturbing the electric field will affect the current, which is measured as the proximity effect. This design has the drawback that no spatial resolution in proximity mode can be implemented within the module. Another similar design using crossing wires is presented by Zhang et al. in [12]. Here, proximity can be measured at the crossing points (taxel/proxel) due to the fringe field, where the measured current drops as a conducting object coupled to ground, such as a human finger, approaches. The same signal can be used to detect tactile measurements as the signal trend reverts when the foam between the wires is compressed. Nonetheless, this solution is not reliable for detecting touch when an object approaches and then retracts without touching the sensor. The detection of objects with floating potential or made of non-conducting materials is not discussed and should pose challenges.

In the domain of consumer-electronics, capacitive tactile and proximity sensing is well established, being ubiquitous in smartphones for example. As in the approaches mentioned above, the devices rely mainly on crossing wires to implement tactile/proximity arrays. In this domain the challenge of achieving a high proximity sensing ranges has been acknowledged, which is also one of the main concerns of this work. As the sensing range can be increased with bigger areas of the electrodes, it has been proposed to dynamically join several taxels/proxels using the switches for wire selection, like the patent by Bernstein et al. [13]. In the case of crossing wires, this has the limitation that only rectangular electrode configurations can be formed. Another example is provided by the patent of Osoinach et al. [14], where proximity electrodes (not crossing wires) in a mutual-capacitive configuration can be joined together dynamically with the same aim. As a drawback, the latter approach does not consider simultaneous tactile measurements. It is worth mentioning that to our knowledge no scientific reports are available where the functionality mentioned in the patents is evaluated.

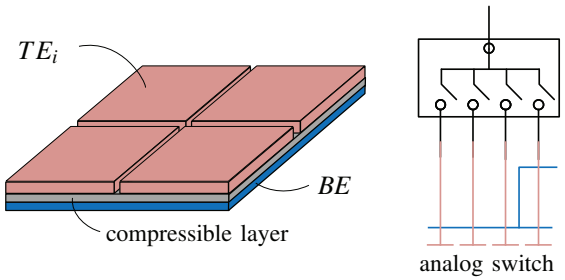

Fig. 2. The assembly of a sensing element for the CTPS together with an analog switch for electrode selection and combination.

Given this background, in this work we propose a novel, versatile capacitive tactile proximity sensor module where the proximity electrodes can be joined together to form arbitrary shapes and which is capable of being interconnected with other modules to build a sensitive skin.

III. System Description

This section is dedicated to presenting the proposed sensor design. First, it is explained how our sensing element is structured, i.e. how the electrodes and dielectric material have to be arranged in order to be able to detect the desired events. Then, the actual circuitry required for driving the sensor and obtaining measurements is explained. Finally, the overall architecture, also comprising digital signal processing, is discussed.

A. Sensing Element

The assembly of the proposed new sensor is shown in Fig. 2. The sensing element – not considering the electronics – consists of two electrode layers that are separated by an insulating, compressible material. There exist a multiplicity of *top electrodes* TE_i, whereby in the example of Fig. 2 there are 4. The *bottom electrode BE* is singular for each module. Using an analog switch, the TE_i can be joined together in an arbitrary way (all possible combinations) to achieve, in an electrical sense, a bigger joint electrode. Provided that A is the total area of all TE_i together, it is possible to implement areas of $\frac{1}{4}A$, $\frac{1}{2}A$, $\frac{3}{4}A$ or A through analog switching. The goal of this design is to be able to drive the sensor in three modes:

- Mode 1: Self-capacitive proximity mode
- Mode 2: Mutual-capacitive tactile mode

- Mode 3: Mutual-capacitive proximity (receive) mode

To perform a measurement in Mode 1, an alternating voltage of a selectable frequency f_{exc} is routed to an arbitrary configuration of the joined TE_i. Simultaneously, using a voltage-follower, the same voltage is applied to *BE* in order to shield the element to its back side. Therefore, undesired capacitive coupling of the sensor to the mechanical structure where it is fixated, e.g. a robot, is avoided. In this self-capacitive configuration the send current is measured. Using time-multiplexing it is possible to take several measurements of different joint TE_i quasi-simultaneously, i.e. in a time delay which is negligible for the desired application. For example, it is possible to poll each TE_i individually, meaning higher spatial resolution, and all TE_i joined, meaning higher reach, in a measurement cycle.

Time-multiplexing is also used to take tactile measurements in Mode 2 in each cycle. In order to obtain these measurements, each TE_i is configured together with *BE* to a mutual-capacitance system. When an external force is applied to the sensing element, the distance of one or more of the TE_i to *BE* is reduced. The foam acts as a spring, which is compressed due to the normal force. In the mutual-capacitance system each of the TE_i acts individually (or jointly if desired) as a send-electrode and *BE* as a receive-electrode, whereby the current is measured at the receiver side.

A third measurement, also in a mutual-capacitive system, is possible, when two or more modules act together, with one group in Mode 1 and the other group in Mode 3. In the first group of modules, a joint configuration of the TE_i is used to generate a send current (Mode 1), which is received by a joint configuration of the TE_i of the second group of modules (Mode 3). An array of sensor modules therefore allows for further methods, such as capacitive tomography. In Mode 3 the receive current is also applied to the *BE* using a voltage follower in order to shield the sensor element.

B. Measurement Circuit

For a proximity range of 0 mm to about 100 mm we observed capacitances of between 10 pF and 0.1 pF. In general, these values are strongly dependent on the area of the electrode and the material of the detected object. Using an analog switch to realize the flexible electrode array increases the parasitic capacitance in the circuit because of the input capacitance of the switch, which makes it hard to measure such a small capacitances directly, i.e. using a low-pass filter circuit. Therefore, we choose a bridge circuit, shown in Fig. 3, to compensate the parasitic capacitance (due to the switch and circuit in general) and the nominal measured capacitance (the offset value due to static coupling with the environment). The bridge voltage gives the capacitance change of the sensor element relative to a reference capacitance. The latter could in principle be calibrated to reach a bridge voltage of 0V at the nominal measured capacitance.

In send-mode (Mode 1), the bridge is actively driven with an exciter signal $\underline{U}_{exc}$ using switch (1) and the send current

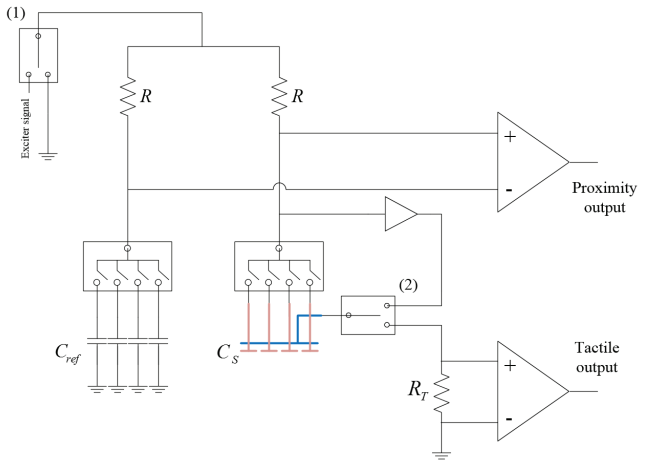

Fig. 3. Bridge circuit for compensation of parasitic capacitances in proximity mode, including the tactile measurement circuit and switches (1) and (2) for reconfiguration

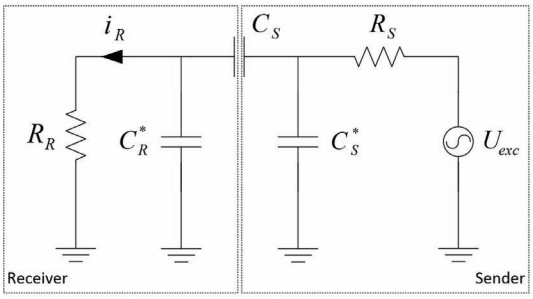

Fig. 4. Equivalent circuit for the mutual-capacitive proximity mode (Mode 3) with one sender and one receiver

is determined by measuring the bridge voltage as shown in (1) and (2)

$$\underline{U}_B = \underline{U}_{exc}\left(\frac{R}{R+Z_{C_s}||Z_{C^*}} - \frac{R}{R+Z_{C_{ref}}||Z_{C^*}}\right) \tag{1}$$

$$\hat{U}_B = \hat{U}_{exc}\left|\left(\frac{1}{1+\frac{1}{j\omega R(C_s+C^*)}} - \frac{1}{1+\frac{1}{j\omega R(C_{ref}+C^*)}}\right)\right| \tag{2}$$

where $\underline{U}_B$ and $\underline{U}_{exc}$ are the complex bridge voltage and the exciter voltage with $\hat{U}_B$ and $\hat{U}_{exc}$ being their respective amplitudes. C_s is the capacitance to be measured. In addition, the *BE* is connected to a voltage follower in order to shield the sensing element using switch (2).

In receive-mode (Mode 3), the onboard exciter signal is disconnected, i.e. switch (1) connects to ground. In this case the measurement resistor acts as a shunt measuring the received current. Again, the *BE* is connected to a voltage follower in order to shield the sensing element using switch (2). The equivalent circuit for a pair of modules in send-receive-mode is illustrated in Fig. 4. The measured shunt voltage at the receiver side is described as follows:

$$\underline{U}_R = \underline{U}_{exc} \left(\frac{Z_{C_R^*} || R_R}{Z_{C_R^*} || R_R + Z_{C_S}} \frac{Z_{C_S^*}}{Z_{C_S} + R_S} \right) \quad (3)$$

$$\hat{U}_R = \hat{U}_{exc} \left| \left(\frac{\frac{C_R^* + R_R}{C_R^* R_R}}{\frac{Z_{C_R^*} + R_R}{Z_{C_R^*} R_R} + Z_{C_S}} \frac{Z_{C_S^*}}{Z_{C_S^*} + R_S} \right) \right| \quad (4)$$

where C_S^* und R_S are the parasitic capacitance and the shunt resistor at the sender side and C_R^* and R_R at the receiver side.

In tactile mode, a direct measurement of the shunt voltage is used to determine the capacitance change given by the deformation of the insulating layer. In this configuration switch (1) connects the exciter signal and switch (2) routes the receive signal through the tactile measurement circuit.

On the digital side, the tactile and the proximity signal are AD-converted with a sample rate of about 1 MHz. After digital filtering, their amplitudes are calculated per discrete Fourier transformation (DFT). The reference signal for the DFT is generated locally and independently of the exciter signal, therefore the phase information of the measured signals is not relevant.

Using the model of a parallel-plate capacitor to describe C_S could help to understand the capacitive system in an ideal case, but such a system is more complex in the field and a corresponding mathematical model could not run effiently on a micro-controller. Therefore we decided to use regression methods to linearize and extract distance information from the calculated amplitude. Here we chose an exponential regression of the form $ax^b + c$ in order to reduce the complexity of the regression model. To get an acceptable residual, a piecewise regression has been implemented, where the measured curve has been divided into two regions, which are fitted with own regressions.

C. Sensor Configuration

The sensor module is fully configurable and the most important configurations are adjustable at runtime by a control register, which can be reached over the bus system, as shown in Fig. 5. This is useful in proximity servoing or environment exploration scenarios, where the range/spatial resolution of proximity measurements can be chosen according to the situation at hand or the frequency of the exciter signal can be adjusted in order to identify the material of obstacles. In summary, the user is able to configure the following: electrode configuration, measurement mode, exciter signal frequency, averaging window size, digital offset compensation and sensor output type (sensor value, calculated distance). Depending on the mentioned configuration the sensor module is able to generate data with a rate between 22 Hz and 380 Hz and a respective latency between 48 ms and 3 ms. For example, the data rate for reading out TE_0,..,TE_4 and TE in Mode 1 for two frequencies is about 40 Hz. The latency is about 26 ms. In any case, the framerate and latency strongly depend on the computing power of the microcontroller used and the desired quality of the measurement.

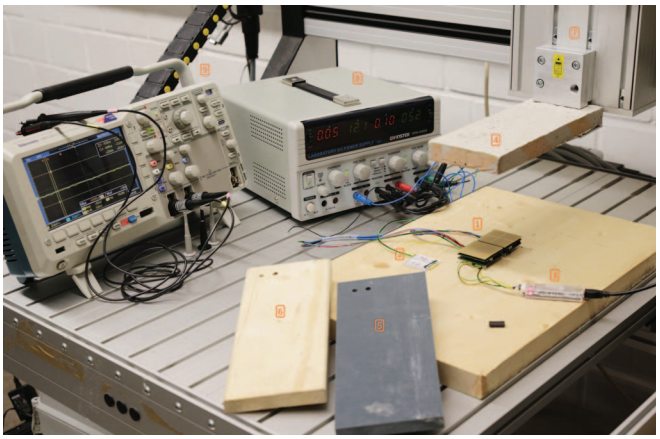

Fig. 6. Experimental Setup

IV. Evaluation

A. Experimental Setup

To evaluate the different modes of the sensor module we used a 1D-robot unit, which holds a test object and moves it in normal direction to the sensor surface with configurable velocity. Regarding to the environment in which the sensor could be installed, we chose test objects made of 4 different materials. The materials are metal (aluminum, grounded), plastic (PVC), dry wood and contraction concrete, as shown in Fig. 6. In the same figure also the LED-Display (2) and the I2C-USB-bridge (3) are shown. The latter is used to read out the sensor data. The sensor module is configured to detect and determine the distance to the test object as follows:

- Amplitude of the exciter signal: 2.5 V
- Frequency of the exciter signal: 100 kHz
- Averaging window: 1
- Electrode configuration: TE_0 - TE_3 separately and the joined top electrodes TE

The dimensions of the objects are provided in Tab. I.

Alu	Wood	PVC	Concrete
120×100×20	240×100×18	240×100×16	240×100×20

TABLE I
Dimension of the test objects in milimeters

B. Proximity and Tactile Modes

For a conducting, grounded object made of aluminum, a self-capacitive proximity measurement was performed over a distance range of 0-60 mm. The expected exponential rise in the curve at smaller distances can clearly be seen in Fig. 7 for the single TE_i as well as for the joined TEs. The measurements also clearly confirm that the measurement range is higher for bigger electrodes.

Since the receive-mode (Mode 3) is more suitable for detection of non-conducting material, the measurement in this mode has been performed for the 4 mentioned materials. To this end, a first sensor module has configured in send-mode and a second one in receive-mode to measure the

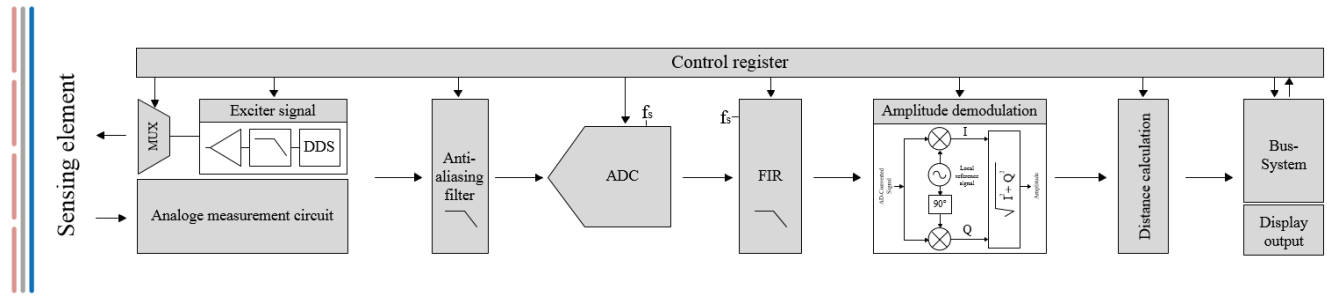

Fig. 5. Functional blocks of the analog and digital components used to measure signals, to control the operation mode of the sensor and to connect it to a bus system

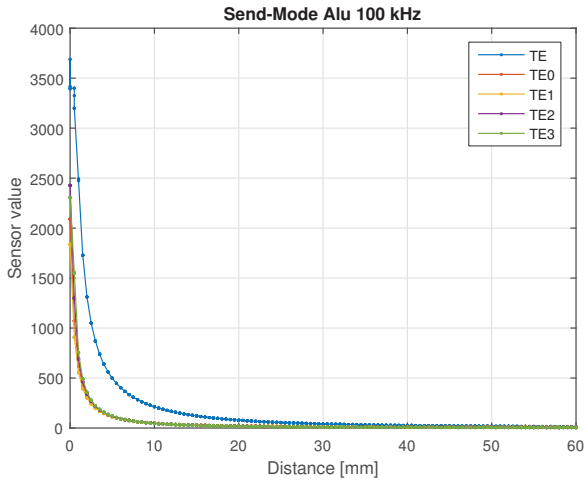

Fig. 7. Measurement curves in send-mode for grounded aluminum

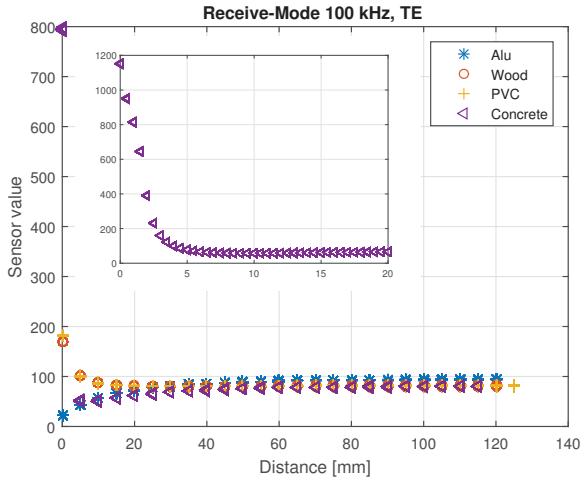

Fig. 8. Measurement curves in receive-mode for different materials

received current with all joint electrodes TE. Non-conducting materials, in this case wood and PVC, act as a dielectric and the capacitance rises as the object approaches the sensor module, due to the fact that their permittivity is greater than that of air. On the other hand, the concrete unexpectedly acted as conductive material, i.e. a drop in the signal can be observed. The probable reason for this behavior is that the concrete was (still) moist during the experiments. The measurement for concrete has been shown with higher resolution as inset in Fig. 7.

To evaluate the tactile mode, a pressure of about 10 N has been exerted on the single top electrodes sequentially by placing a weight on them. The measurement curves in Fig. 9 shows the resulting 4 peaks, which have different amplitude, although the electrodes experienced the same amount of pressure. This is due to the fact that isolation layer (foam) does not have the same area under top electrodes in the prototype, which lead to different deformation by the same amount of pressure. The exact relation between the pressure and the sensor value have not been analyzed, but will be done in the future.

C. Repeatability

One of the most important criterions of a measurement system is how repeatable its output is. We therefore evaluated the repeatability of the proximity mode of our module for different configurations. Fig. 10 shows 5 exemplary measurement curves in send-mode, which have been recorded after waiting a variable amount of time (10 minutes-1 hour).

D. Distance Regression

As mentioned before, we chose the piecewise continuous regression method rather than a physical model to get a linear relationship between sensor value and the real distance in send-mode. A measurement curve has been recorded and splitted into two regions. The regions have been fitted with the function $ax^b + c$ using MATLAB's regression toolbox. Fig. 11 and Fig. 12 show the regressions (upper figures) and their residual (bottom figures) of both regions, from 0 mm to 20 mm and from 20 mm to 100 mm. When programmed into the firmware, the sensor module is able to determine the region and to choose the corresponding parameter of the regression.

As an example, Fig. 13 shows the online calculated distance for aluminum. Again, it is clear how much smaller the measurement range of the single top electrodes TE_0

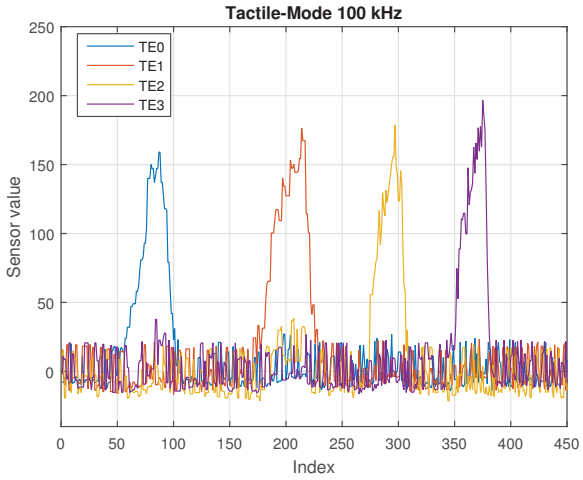

Fig. 9. Measurement curves in tactile-mode

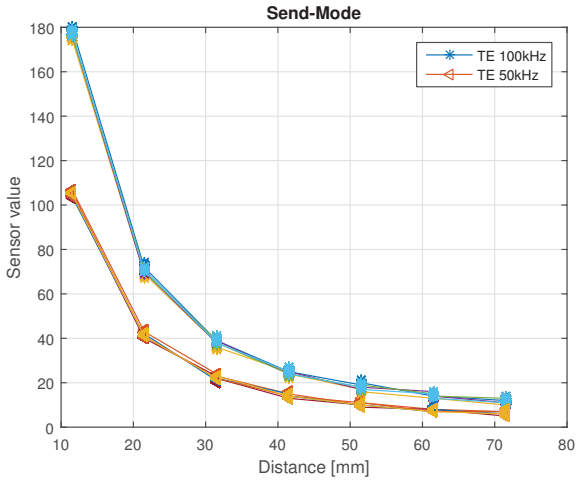

Fig. 10. Measurements for repeatability

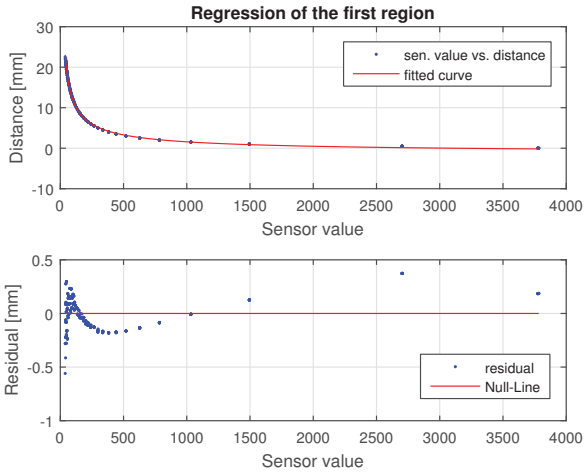

Fig. 11. Example regression for a higher sensor value range (lower distances)

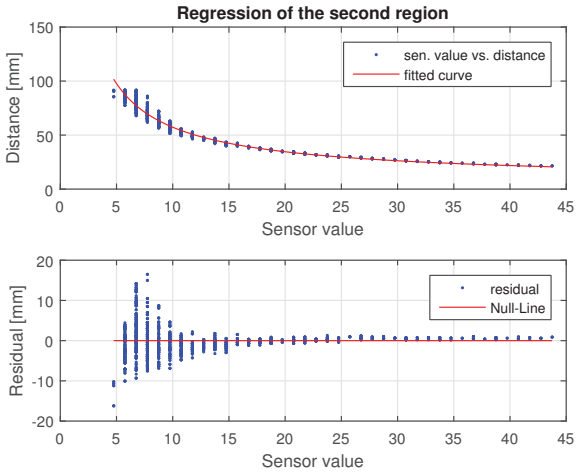

Fig. 12. Example regression for a lower sensor value range (higher distances)

- TE_3 is against the joint electrode TE. The TE curve shows that the gaps between the calculated distance, which determine the resolution, rise at higher distances. This is a result of the exponential function, which in this case decreases the resolution of the measurement by amplifying the equidistance gaps by a.

E. LED-Display

As a feature realizing intuitive feedback for the human, we implemented a display for the sensor values in a 2×2 array of LEDs that shows them in a heat map, as seen in Fig. 14. Future iterations of the sensor will include the LEDs directly on the PCB.

V. Conclusions and Future Work

In this work we have shown a novel sensor for detecting tactile and proximity events using a capacitive measuring principle. Its fields of application are robotics and consumer-electronics. The first contribution is an electro-mechanical design of the sensing element, with which it is possible to implement a dynamic spatial resolution in the tactile and proximity mode simultaneously. The trade-off between electrode size (spatial resolution) and proximity sensing range is addressed. The design of a corresponding electrical circuit that drives the sensor completes the conceptual discussion. Then, a prototypical implementation of the sensor, for which measurement results of the diverse operation modes are discussed, was shown.

One of the major challenges in the implementation of the sensor was the compensation of parasitic capacitances due to the analog switch and other components in the circuit. The proposed solution is the measurement-bridge that was discussed. While showing a good performance, the implementation is costly (economically, and regarding space on the PCB) and currently we are looking into alternatives. The sensing range of of the tactile mode also leaves room for improvement. Here, approaches consider different dimensioning of the passive electrical components. The connection

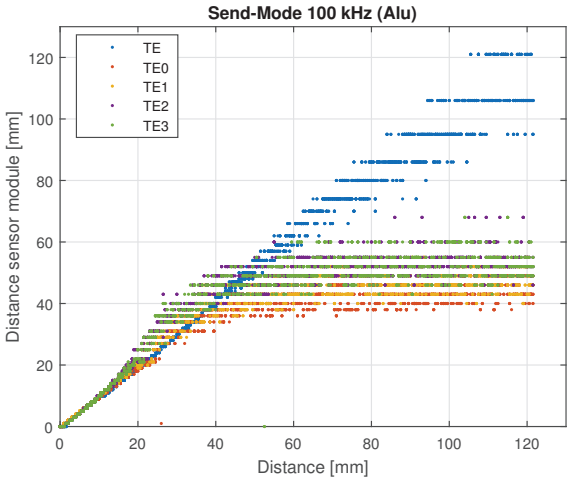

Fig. 13. Example distance output of the sensor

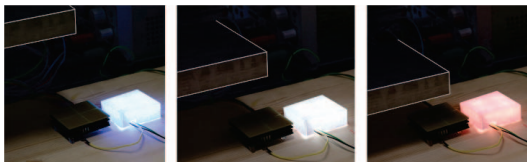

(a) An aluminum plate approaching from top, perceived by all top electrodes joined

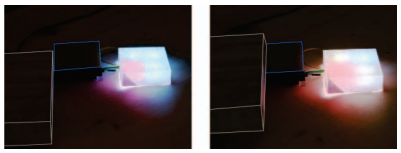

(b) An aluminum plate approaching from top/side, perceived by all top electrodes individually

Fig. 14. The output of the proximity mode displayed on a 2×2 array of LEDs that is located next to the sensor module (the borders of the aluminum plate are highligthed for clarity)

of two or more sensor modules through a bus system was tested, but limits on the data rate and its relation to the number of modules were not yet evaluated.

A definite direction for future work will be the integration of this new generation of sensor modules into grippers and as skin on the exterior of robot links. We expect that the performance of our approaches for manipulation and HRI can be significantly improved due to reduced latency, increased spatial resolution and additional functionality. Still, we see the sensor as complementary sensing system to other systems, e.g. optical sensors (IR, RGBD-cameras, etc.).

References

[1] D. Göger, M. Blankertz, and H. Wörn, "A Tactile Proximity Sensor," in *IEEE Sensors 2010*, 2010, pp. 589 –594.

[2] D. Göger, H. Alagi, and H. Wörn, "Tactile Proximity Sensors for Robotic Applications," in *International Conference on Industrial Technology (ICIT)*, 2013.

[3] S. Escaida Navarro, M. Marufo, Y. Ding, S. Puls, D. Göger, B. Hein, and H. Wörn, "Methods for Safe Human-Robot-Interaction Using Capacitive Tactile Proximity Sensors," in *Intelligent Robots and Systems (IROS), 2013 IEEE/RSJ International Conference on*, 2013, pp. 1149–1154.

[4] S. Escaida Navarro, M. Schonert, B. Hein, and H. Wörn, "6D Proximity Servoing for Preshaping and Haptic Exploration using Capacitive Tactile Proximity Sensors," in *Intelligent Robots and Systems (IROS), 2014 IEEE/RSJ International Conference on*, 2014, pp. 7–14.

[5] S. Escaida Navarro, F. Heger, F. Putze, T. Beyl, T. Schultz, and B. Hein, "Telemanipulation with Force-based Display of Proximity Fields," in *Intelligent Robots and Systems (IROS), 2015 IEEE/RSJ International Conference on*, 2015, pp. 4578–4574.

[6] Jan Hergenhan and Jacqueline Rutschke and Michael Uhl and Stefan Escaida Navarro and Björn Hein and Heinz Wörn, "A Haptic Display for Tactile and Kinesthetic Feedback in a CHAI 3D Palpation Training Scenario," in *2015 IEEE Conference on Robotics and Biomimetics (ROBIO 2015)*, 2015.

[7] N. Wettels, J. Fishel, and G. Loeb, "Multimodal tactile sensor," in *The Human Hand as an Inspiration for Robot Hand Development*, ser. Springer Tracts in Advanced Robotics, R. Balasubramanian and V. J. Santos, Eds. Springer International Publishing, 2014, vol. 95, pp. 405–429.

[8] P. Mittendorfer and G. Cheng, "Humanoid multimodal tactile-sensing modules," *Robotics, IEEE Transactions on*, vol. 27, no. 3, pp. 401–410, June 2011.

[9] K. Koyama, H. Hasegawa, Y. Suzuki, A. Ming, and M. Shimojo, "Pre-shaping for various objects by the robot hand equipped with resistor network structure proximity sensors," in *Intelligent Robots and Systems (IROS), 2013 IEEE/RSJ International Conference on*, Nov 2013, pp. 4027–4033.

[10] K. Koyama, Y. Suzuki, A. Ming, and M. Shimojo, "Grasping control based on time-to-contact method for a robot hand equipped with proximity sensors on fingertips," in *Intelligent Robots and Systems (IROS), 2015 IEEE/RSJ International Conference on*, 2015.

[11] H.-K. Lee, S.-I. Chang, and E. Yoon, "Dual-mode capacitive proximity sensor for robot application: Implementation of tactile and proximity sensing capability on a single polymer platform using shared electrodes," *Sensors Journal, IEEE*, vol. 9, no. 12, pp. 1748–1755, 2009.

[12] B. Zhang, Z. Xiang, S. Zhu, Q. Hu, Y. Cao, J. Zhong, Q. Zhong, B. Wang, Y. Fang, B. Hu, J. Zhou, and Z. Wang, "Dual functional transparent film for proximity and pressure sensing," *Nano Research*, vol. 7, no. 10, pp. 1488–1496, 2014.

[13] J. T. Bernstein, "Capacitive sensor panel having dynamically reconfigurable sensor size and shape," U.S. Patent US000 008 390 597B2, 2013.

[14] B. Osoinach, "Device with proximity detection capability," U.S. Patent US000 008 115 499B2, 2012.